A model for predicting coupled heat and mass transfers in unsaturated partially frozen soil

S. G. Giakoumakis
Laboratory of Rural Technology, National Technical University of Athens, Athens, Greece

A one-dimensional model is used for simulating coupled heat and mass transfers in a vertical porous medium column, with the upper end subjected to a negative temperature. The model can predict accurately both temperature and total water content profiles along the column, provided that both heat- and mass-conservation equations are solved simultaneously. On the contrary, when only heat transfer equation is solved, the position of the moving freezing front (isothermal of 273.16°K), is systematically underestimated. Moreover, it was shown that the commonly used surface-tension viscous-flow theory for estimating the temperature-dependent soil hydraulic properties (i.e., matric potential versus liquid water content, $h[\Theta_l]$, and hydraulic conductivity versus liquid water content, $K[\Theta_l]$), when combined with the model, fails to describe satisfactorily the evolution of the freezing process.

Keywords: heat and mass transfers; surface-tension viscous-flow theory; medium hydraulic properties; soil freezing

Introduction

Both thermal and moisture regimes in unsaturated, partially frozen soils influence simultaneously moisture movement and water storage in the frozen region. Considerable effort has been made in attempting to define the mechanisms of water transport from the unfrozen to the frozen zone. It was proved that moisture migration generated by the freezing process is continuous, as long as both cryogenic suction and temperature gradients are developed and an external water supply is available (Vauclin and Giakoumakis 1987).

This phenomenon, with or without frost heaving, has important consequences in hydrology, foundation and highway engineering and agriculture, in both seasonal frost and permafrost areas.

Many theoretical approaches have been developed to correlate water migration to driving suction and thermal gradients or to hydraulic and thermal soil properties (Aguirre-Puente and Fremond 1975; Hoekstra 1966; Morel-Seytoux 1979; Miller 1980). Moreover, many mathematical models have been proposed to describe heat and water flow in freezing soils (Aguirre-Puente et al. 1978; Guymon and Luthin 1974; Kay et al. 1976; Kennedy and Lielmez 1973).

In this study, the mathematical model is solved numerically by the finite-difference method, using an implicit scheme. The model considers two different approaches for estimating variations of the soil hydraulic properties with temperature: the surface-tension viscous-flow theory (STVF) and the Gain factor empirical model (Nimmo and Miller 1986). Simulation yields temperature and total water content (liquid and ice) profiles, which were compared with experimental data obtained on a vertical column of unsaturated fine/medium sand, and submitted to various initial and boundary conditions including freezing on soil surface. It was shown that the model can predict satisfactorily the physical process (i.e., evolution of temperature and total water content profiles along the column, liquid-water transport from the unfrozen to the frozen zone of the soil, and position of the moving freezing front), provided that both conservation equations are solved simultaneously and variations with temperature of the soil hydraulic properties are quantified via the Gain factor empirical model. On the contrary, when STVF theory is used or/and only temperature conservation equation is solved, the model fails to predict accurately the overall processes related to soil freezing.

Mathematical model

The mathematical formulation of simultaneous heat and mass transport in a partially frozen, unsaturated porous medium is based on the system of heat- and mass-conservation equations proposed by Harlan (1973). Because of the strong nonlinearity of these equations, only numerical techniques are used for solving the problem, provided that both hydraulic and thermal medium properties under unfrozen and frozen conditions are previously determined. The model used is based on several assumptions, some of which have been validated experimentally:

1. The porous medium is considered to be homogeneous, isotropic and rigid (no deformation of the solid matrix occurs during freezing).
2. Both air and ice phases are assumed to be at the atmospheric pressure.
3. The water is chemically pure. No simultaneous solutes transport occurs.

Address reprint requests to Dr. Giakoumakis at the Laboratory of Rural Technology, National Technical University of Athens, 9, Iroon Polytechniou Str.-15780, Athens, Greece.

Received 6 April 1993; accepted 29 November 1993

4. Capillary theory of the water transport is valid, both in the unfrozen and frozen zones. Especially in the frozen zone, the cryogenic suction developed, is a function of the unfrozen water content, which in turn, is a function of the temperature decrease below 273.16K, (0°C), (freezing point depression).
5. In the heat transport equation, the convective term is considered negligible compared with the conductive term. Besides, it was shown experimentally that the vapor phase contribution to mass transport is of negligible magnitude (Fuchs et al. 1978; Taylor and Luthin 1978).
6. Local thermodynamical equilibrium exists between liquid water and ice phases (Kay and Groenevelt 1974).

Under the foregoing assumptions, the one-dimensional coupled heat-fluid flow transport equations, are derived.

Mass-transport equation:

$$C_h(\Theta_1, T)\theta h/\theta t = \partial/\partial z[K(\Theta_1, T)(\partial h/\partial z - 1) + D_T(\Theta_1, T)\partial T/\partial z] + \Delta S \quad (1)$$

with $C_h(\partial_1, T) = \partial\Theta_1/\partial h_T$ and $\Delta S = -(\rho_g/\rho_1)\partial\Theta_g/\partial t$

Equation 1, is a slightly modified version of the one proposed by Harlan. Namely, it also takes into account the liquid moisture flux in the unsaturated zone induced by thermal gradients. According to Philip and De Vries (1957), the thermal liquid diffusivity coefficient on the right hand side of Equation 1 can be expressed as follows:

$$D_T(\Theta_1, T) = K(\Theta_1, T)h(\Theta_1, T)\gamma(T) \quad (2)$$

with $\gamma(T) = 1/\sigma(T)d\sigma/dT$

Heat-transport equation:

$$C_{ap}\partial T/\partial t = \partial/\partial z[\lambda(\partial T/\partial z)] \quad (3)$$

with $C_{ap} = C^* - R_g L_{1g}\partial\Theta_g/\partial T = C^* + R_1 L_{1g}\partial\Theta_1/\partial T$

Equation 3 can also be written

$$(C^*\partial T/\partial t - R_1 L_{1g}\partial\Theta_g/\partial t) = \partial/\partial z[\lambda(\partial T/\partial z)] \quad (4)$$

Notation

a_T	thermal diffusivity of the porous medium, L^2T^{-1}
C_{ap}	apparent volumetric heat capacity, $ML^{-1}T^{-2}K^{-1}$
C^*	volumetric heat capacity of the porous medium, $ML^{-1}T^{-2}K^{-1}$
C_h	soil capillary capacity, L^{-1}
C_i	volumetric heat capacity of the ith constituent, $ML^{-1}T^{-2}K^{-1}$
D_T	thermal liquid diffusivity coefficient, $L^2T^{-1}K^{-1}$
g	acceleration of gravity, LT^{-2}
G_h, G_k	Gain factors
h	soil water matric potential, L
H	total soil water potential at hydrostatic equilibrium, L
h_{ext}	external pressure at the bottom of the column, L
h_L	soil water matric potential at the bottom of the column, L
h_{cr}	frozen soil cryogenic suction, L
$h(\Theta_1)$	matric potential versus liquid water content function, L
$h^*(\Theta_1)$	soil matric potential normalized function, $M^{-1}LT^2$
I	impedance factor
K	soil hydraulic conductivity, LT^{-1}
K_g	frozen soil hydraulic conductivity, LT^{-1}
$K(\Theta_1)$	hydraulic conductivity versus liquid-water content function, LT^{-1}
$K^*(\Theta_1)$	soil hydraulic conductivity normalized function, L^3T^{-2}
L	column's height, L
L_{lg}	latent heat of fusion of water, L^2T^{-2}
l_p	thickness of the porous plate at the bottom of the column, L
q_m	liquid water flux, LT^{-1}
T	temperature, K
T_0	273.16K (0°C), freezing point of free water
t	time, T
V_l	cumulative volume of liquid water entered into the column, L^3
z	vertical coordinate (z-axis is positively oriented downward), L
Z_f	freezing front location with respect to the column's surface, L

Greek letters

α	impedance of the porous plate, T^{-1}
γ	temperature coefficient of surface tension, K^{-1}
ΔS	rate at which liquid water is converted to ice per unit volume per unit time, T^{-1}
$\Delta T = T_0 - T$	freezing point depression relative to the freezing point of free water, K
Θ	total volumetric water (liquid water and ice) content, L^3L^{-3}
Θ	volumetric content of the ith constituent of the porous medium, L^3L^{-3}
Θ_g	volumetric ice content, L^3L^{-3}
Θ_l	volumetric liquid water content, L^3L^{-3}
Θ_s	volumetric water content at saturation, L^3L^{-3}
κ_i	empirical weighing factor of the ith constituent
λ	thermal conductivity of the porous medium, $MLT^{-3}K^{-1}$
λ_i	thermal conductivity of the ith constituent, $MLT^{-3}K^{-1}$
ν	kinematic viscosity of liquid water, L^2T^{-1}
ρ_l, ρ_g	densities of liquid and ice fractions, respectively, ML^{-3}
σ	surface tension at the liquid water-air interface, MT^{-2}
σ_{lg}	surface tension at the liquid water-ice interface, MT^{-2}
ω	exponent

Subscripts

ap	apparent
i	ith medium's constituent
Tre	at reference temperature
T	at temperature T

As can be observed from Equations 1 and 4, the coupling term $\partial\Theta_g/\partial t$ expresses the decrease of the liquid water in the frozen zone, with respect to time (phase change liquid water to ice).

Experimental study

Experiments were conducted in a vertical soil column, packed into a Plexiglas cylinder 55 cm high, with an inside diameter of 6 cm (Giakoumakis 1987). Water flow into and from the soil column was realized through a ceramic porous plate (impedance $\alpha = 0.001\ s^{-1}$, thickness $l_p = 0.2$ cm), placed at the bottom of the cylinder, allowed it to be connected with an external constant piezometric head.

Hollow brass liquid circulation plates connected to cryogenic baths were placed at both ends of the column to apply a constant temperature at each end.

To obtain a constant thermal gradient along the column during nonisothermal experiments or for establishing isothermal conditions all over the cylinder (case of isothermal experiments), a lateral dynamic insulation system, involving 10 independent parallelepipedic cells (36 × 18 × 5.5 cm), was used. Each cell contained appropriate devices (serpentine-shaped exchanger connected to the cryogenic baths and a heating electrical resistance), allowing adjustment of the air cell temperature to the soil temperature at the same depth. Furthermore, the air temperature in each cell was kept as uniform as possible by means of an electrical fan.

The system was controlled automatically by a Zilog Z-80 microcomputer in such a way that the difference between the air and soil temperatures never exceeded ±0.1K, this difference kept constant, even for long experimental durations (Giakoumakis 1984).

The variables of state, namely, air and soil temperatures, T_a and T_s, total (liquid water and ice) volumetric water content, Θ, as well as matric potential, h, were measured at 10 different column depths, using specific devices (Albergel 1984; Vachaud and Thony 1971): platinum resistances, gamma-ray attenuation (comprised a 300-mCi Am 241 source and a scintillation detector, both positioned on a moving platform) and differential pressure transducers, respectively (Figure 1). All measured data were stored by the microcomputer at constant time intervals.

The soil used was an alluvial fine/medium sand (0.05–0.5 mm) without organic matter, consisting mainly of quartz (55 percent) and of other minerals (45 percent). After soil's packing into the cylinder, medium's uniformity was verified by determining the bulk density distribution profile, using the gamma-ray attenuation system (mean value: 1.63 ± 0.0127 gr/cm³).

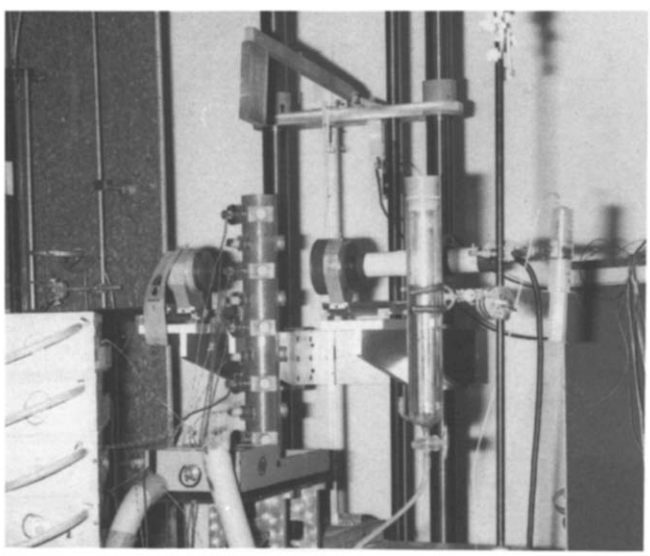

Figure 1 General view of the experimental set-up

Two types of experimental tests were carried out.

1. Isothermal experiments comprising wetting and drying cycles performed at 293.16, 281.16 and 276.16K, kept constant in time. These experiments allowed to determine the soil hydraulic properties $h(\Theta_1)$ and $K(\Theta_1)$ at each one of the three temperatures as well as their variations with temperature.
2. Nonisothermal experiments, with different initial and boundary thermal and moisture conditions. Two cases were considered.
   a. Nonfreezing conditions: in this case, the soil thermal diffusivity and conductivity were determined as functions of liquid-water content, Θ_1.
   b. Freezing conditions (negative temperatures applied at the soil surface): this allowed to study the penetration of a moving freezing front into the unsaturated soil.

Medium properties

To solve the heat- and mass-transfer equations, soil hydraulic and thermal properties have to be known. For this study, both experimental and theoretical approaches have been used for determining medium properties under unfrozen and frozen conditions.

Hydraulic properties of the unfrozen soil

Medium hydraulic properties are expressed by the characteristic functions matric potential versus water content, $h(\Theta_1)$, and hydraulic conductivity versus water content, $K(\Theta_1)$, which are closely dependent on temperature (Haridasan and Jensen 1972; Hopmans and Dane 1986; Novak 1975). On the contrary, it has been proved that the normalized forms $h^*(\Theta_1)$ and $K^*(\Theta_1)$ of these functions are independent of temperature (Giakoumakis and Tsakiris 1991).

$$h_T(\Theta_1)/\sigma_{apT} = h_{Tre}(\Theta_1)/\sigma_{Tre} = h^*(\Theta_1) \tag{5}$$

$$K_T(\Theta_1)\nu_{apT} = K_{Tre}(\Theta_1)\nu_{Tre} = K^*(\Theta_1) \tag{6}$$

where $h_T(\Theta_1)$, $K_T(\Theta_1)$ and $h_{Tre}(\Theta_1)$, $K_{Tre}(\Theta_1)$ are the soil characteristic functions at temperatures T and T_{re}, respectively, whereas σ_{Tre} and ν_{Tre} are the surface tension and kinematic viscosity values at the reference temperature. Moreover, σ_{apT} and ν_{apT} are the "apparent" surface tension and kinematic viscosity at temperature T, given by

$$\sigma_{apT} = \sigma_{Tre}(1 + G_h(\Theta_1)\{[\sigma_T/\sigma_{Tre}] - 1\}) \tag{7}$$

$$\nu_{apT} = \nu_{Tre}/(1 - G_k(\Theta_1)\{1 - [\nu_{Tre}/\nu_T]\}) \tag{8}$$

where G_h and G_k ($G_h, G_k \geq 1$) are the Gain factors corresponding to $h(\Theta_1)$ and $K(\Theta_1)$, respectively, whereas σ_T and ν_T are the surface tension and kinematic viscosity at temperature T. Equations 7 and 8, for $G_h = G_k = 1$, result in the well-known STVF theory equations ($\sigma_{apT} = \sigma_T$, $\nu_{apT} = \nu_T$).

In this work, the experimental research (isothermal experiments involving infiltration and drainage cycles at 293.16, 281.16 and 276.16K), has shown for the soil studied (fine/medium sand) that the STVF method is not adequate to explain the observed variations in both $h(\Theta_1)$ and $K(\Theta_1)$ functions, with temperature. This may be attributed to the temperature effect on the entrapped air in the soil matrix (Chahal 1964; Peck 1960) and/or the presence of surface active

contaminants at the air-water interfaces (Wilkinson and Klute 1962). As for the $K(\Theta_1)$ function, Constantz (1982) claimed that discrepancies between measured and STVF predicted values could be explained by the higher temperature coefficient of kinematic viscosity of capillary water compared with free water. Moreover, Nimmo and Miller (1986) showed that the STVF approach is more appropriate to predict $h(\Theta_1)$ and $K(\Theta_1)$ changes with temperature for coarse soils (e.g., coarse sand) than for fine-textured soils.

Considering as reference temperature $T_{re} = 293.16K$ and using the data collected at the three temperatures, experimental values of G_h and G_k were derived at different water contents, Θ_1.

$$G_h(\Theta_1) = ([h_T(\Theta_1)/h_{Tre}(\Theta_1)] - 1)/([\sigma_T/\sigma_{Tre}] - 1) \quad (9)$$

$$G_k(\Theta_1) = (1 - [K_T(\Theta_1)/K_{Tre}(\Theta_1)])/(1 - \nu_{Tre}/\nu_T) \quad (10)$$

Thus, the apparent surface tension and kinematic viscosity, σ_{ap} and ν_{ap}, were calculated at 281.16 and 276.16K (Equations 7 and 8) and the normalized experimental points $h_T(\Theta_1)/\sigma_{apT}$ and $K_T(\Theta_1)\nu_{apT}$, were determined (Equations 5 and 6). Finally, least-squares fits for the $h^*(\Theta_1)$ and $K^*(\Theta_1)$ functions were obtained (Figures 2a and b).

The form of the least-squares equations, as well as their fitting parameters, are given in Table 1 (Equations T1.1 and T1.2/parameter set 1). For comparison reasons, in the same table are also presented the fitting parameters corresponding to the least-squares fits of $h_T(\Theta_1)/\sigma_T$ and $K_T(\Theta_1)\nu_T$, experimental points (STVF method—Equations T1.1 and T1.2/parameter set 2). The STVF normalizations are illustrated in Figures 3a and b. By comparing the mean quadratic error (MQE) values of the normalized $h^*(\Theta_1)$ fitted curves, as well as the correlation coefficient (CC) of the $K^*(\Theta_1)$ fitted curve (Gain factor approach), with the MQE and CC values corresponding to the normalizations obtained by the STVF method, it is obvious that, when normalizations are performed through Gain factor's model, MQE values are lower, whereas the CC value is much higher (Table 1).

Hydraulic properties of the frozen soil

In the frozen soil the cryogenic suction corresponding to the unfrozen water increases (in absolute value) as the quantity of water is reduced by ice formation. The cryogenic suction, h_{cr}, can be related to the freezing point of the pore water, ΔT, via Clausius-Clapeyron equation.

$$h_{cr}(\Delta T) = [L_{lg}/(gT_0)]\Delta T \quad (11)$$

Equation 11 has been validated experimentally for different soil types (Williams 1964b).

For a granular medium (sandy soil), the capillary interpretation of the cryogenic suction and the hypothesis that there is an analogy between the unfrozen and frozen soil characteristic functions $h^*(\Theta_1)$ (Equation 5) and $h_{cr}(\Delta T)$, respectively, lead to the following equation (Koopmans and Miller 1966):

$$h_T(\Theta_1)/\sigma_{apT} = h_{cr}(\Delta T)/\sigma_{lg}(\Delta T) = h^*(\Theta_1) \quad (12)$$

The surface tension at the liquid water-ice interface, σ_{lg}, can be estimated by the equation (Hesstvedt 1964)

$$\sigma_{lg}(\Delta T) = 31.7(1 + 0.93\,10^{-2}\,\Delta T), \text{ in dyn/cm} \quad (13)$$

Taking account of the Equation 11, Equation 12 becomes

$$h_T(\Theta_1)/\sigma_{apT} = [L_{lg}/(gT_0)]\,\Delta T/\sigma_{lg}(\Delta T) = h^*(\Theta_1) \quad (14)$$

Equation 14 expresses the relationship between the unfrozen water content, Θ_1, and the freezing point depression, ΔT.

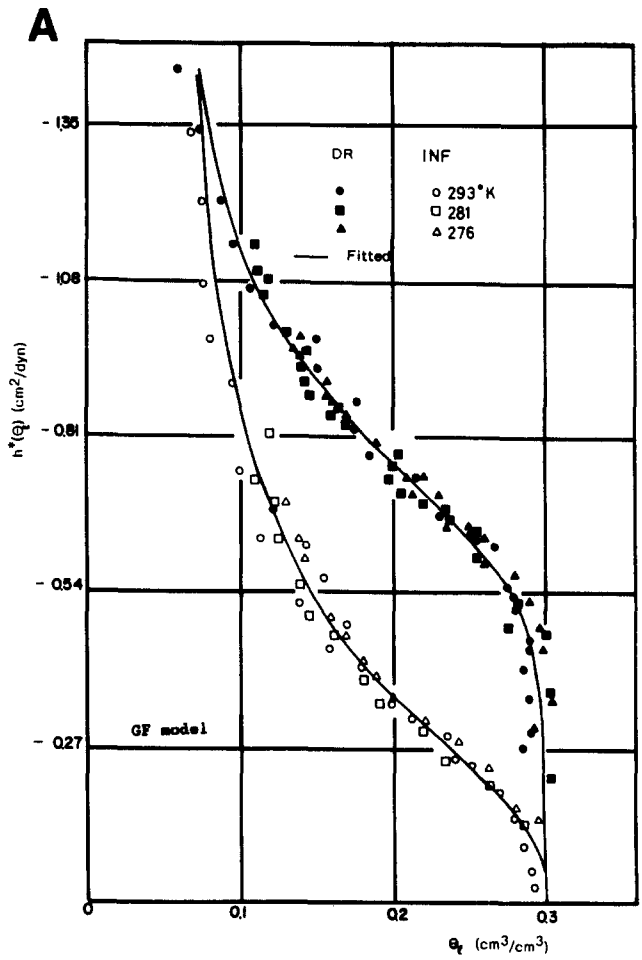

Figure 2 Normalized functions $h^*(\theta_1)$ and $K^*(\theta_1)$: Gain factor model

Table 1 Analytical expressions for $h^*(\theta_1)$ and $K^*(\theta_1)$ normalized curves

$$\Phi = [1/(1 + (a|h^*|)^n]^m \text{ for } h \leq 0 \quad (T1.1)$$
$$\Phi = 1.0 \text{ for } h > 0$$

where $\Phi = (\theta_1 - \theta r)/(\theta s - \theta r)$, $m = 1 - 1/n$

$$K^*(\theta_1) = c(\theta_1/\theta s)^b \quad (T1.2)$$

	Set 1/Gain factor model		Set 2/STVF method	
Parameters	Drainage	Infiltration	Drainage	Infiltration
θs	0.30	0.30	0.30	0.30
θr	0.06	0.06	0.06	0.06
a (dyn cm^{-2})	1.289	3.11	2.81	2.82
n	5.39	2.75	5.28	2.53
MQE[a] (cm^2 dyn^{-1})	7.1×10^{-2}	0.108	8.8×10^{-2}	0.235
c (cm^{3}h^{-2})	444.01		332.1	
b	3.01		3.284	
CC[b]	0.91		0.78	

[a] Mean quadratic error.
[b] Correlation coefficient.

Because of the fact that no experimental investigations have been carried out for determining the $\Theta_1(\Delta T)$ relationship for the soil studied, Equation 14 allowed to estimate the amount of unfrozen water as a function of the temperature decrease below 273.16K (0°C). This relationship is illustrated in Figure 4. From this figure, the steep decrease of the unfrozen water content Θ_1 with a relative small decrease in ΔT can be seen.

The presence of the ice in the frozen zone restricts liquid water movement and, hence, reduces considerably medium's conductive ability. Different methods, consisting in the use of specific permeameters, have been developed for measuring the hydraulic conductivity of the frozen soil (Aguirre-Puente and Gruson 1983; Burt and Williams 1976; Miller et al. 1975).

In the present study, the hydraulic conductivity of the frozen soil K_g, as a function of the unfrozen water content Θ_1, is calculated by the equation

$$K_g(\Theta_1) = I(\Theta_g)K^*(\Theta_1) \quad (15)$$

In Equation 15, the parameter I is an impedance factor, which is assumed to be a function of the volumetric ice content, Θ_g (Jame and Norum 1980).

$$I(\Theta_g) = 10^{-\omega\theta g} \quad (16)$$

ω is the exponent depending on soil type.

Thermal properties of the unfrozen soil

In this study, the soil thermal coefficients, λ and C^* (thermal conductivity and volumetric heat capacity, respectively), are calculated by the well-known De Vries (1963) theoretical model. According to this model, λ and C^* are given by

$$\lambda = \sum_{i=1}^{n} (\theta_i k_i \lambda_i)/(\theta_i k_i) \quad (17)$$

$$C^* = \sum_{i=1}^{n} (C_i \theta_i) \quad (18)$$

where

i = index denoting medium's substance (quartz, other minerals, organic matter, liquid water, ice or gaz)
n = maximum number of substances

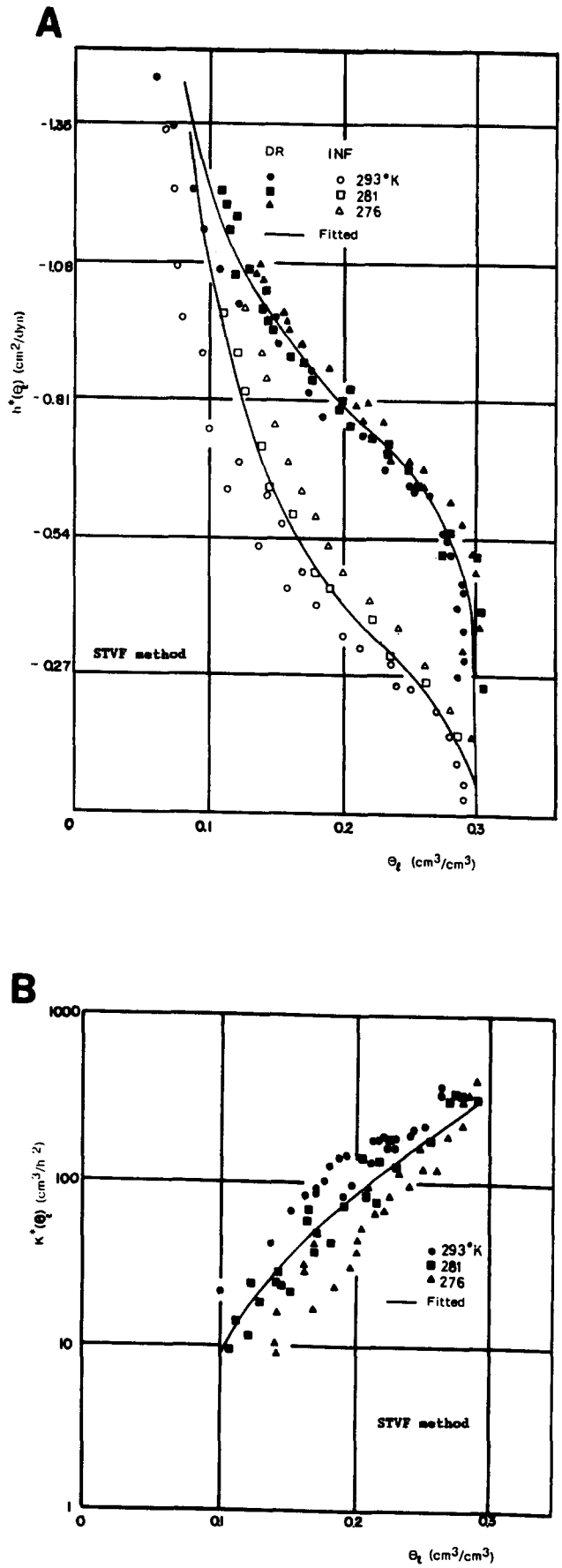

Figure 3 Normalized functions $h^*(\theta_1)$ and $K^*(\theta_1)$: STVF method

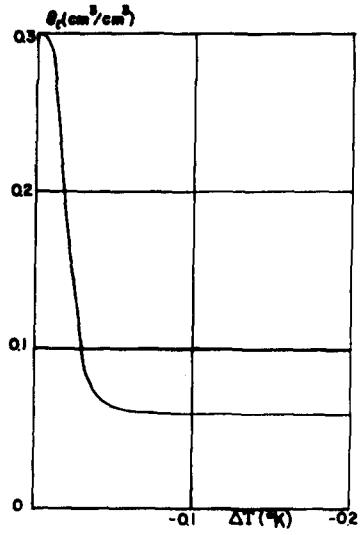

Figure 4 Unfrozen water content versus freezing-point depression

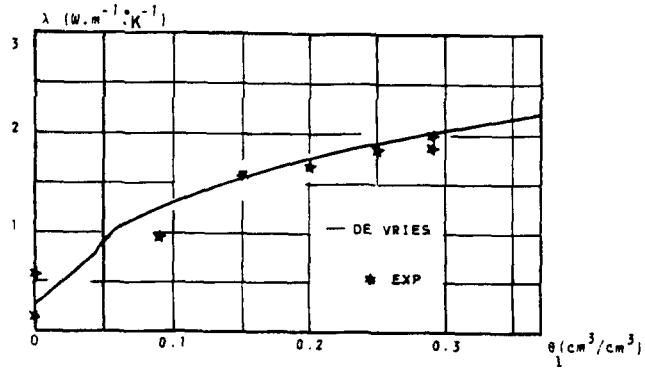

Figure 5 Thermal conductivity versus liquid-water content for the unfrozen soil

The predictive ability of this model was tested as follows. For the soil studied, the thermal diffusivity a_T, which is equal to the ratio λ/C^*, was determined as a function of liquid water content Θ_1, by analyzing temperature profiles along the soil column, during nonisothermal transient experimental tests, according to a methodology proposed by Vauclin et al. (1978). Then, thermal conductivity, $\lambda = a_T C^*$, was derived by computing C^* from Equation 18.

The so determined values of λ for the unfrozen soil and those calculated from the De Vries model (Equation 17) are illustrated in Figure 5. It can be concluded that there is a good agreement between experimental data and predicted values of λ. It should be mentioned that no significant temperature dependence of λ was observed.

Thermal properties of the frozen soil

Thermal conductivity and heat capacity of the frozen soil were calculated by using the corresponding De Vries equations including the ice as an additional component of the system. Moreover, the latent heat of fusion delivered during the phase-change liquid water to ice is involved in the so-called apparent volumetric heat capacity, C_{ap}, (Equation 3). This coefficient can be determined experimentally by using calorimetric methods (Williams 1964a). In the present study, the apparent heat capacity is estimated by adding to the heat capacity of the medium, C^* (Equation 18, ice phase included), the term: $\rho_l L_{lg} \partial\Theta_l/\partial T$, in which the derivative $\partial\Theta_l/\partial T$ is the slope of the characteristic curve $\Theta_l(\Delta T)$ at any ΔT (Figure 4). The relationship $C_{ap}(\Delta T)$ is shown in Figure 6.

From this figure, it is obvious that a very small decrease in temperature below 273.16K (0°C), causes a sharp rise in the heat capacity of the soil. For comparison reasons, in the same figure, the dashed line represents the term C^* only, whereas the solid line represents the latent heat and C^* terms together (apparent heat capacity).

Results and discussion

In this work, two nonisothermal experimental tests (hereafter referred as tests A and B), including freezing on soil surface, have been simulated. These experiments correspond to different initial and boundary hydraulic and thermal conditions applied on the soil column (Table 2).

It should be mentioned that the bottom of the column was connected to a Mariotte-type external reservoir of water, which was positioned at a constant depth (different for each experiment), with respect to the soil surface. This reservoir is graduated in cm^3, and volumes of water flowing into the column could be readily estimated (Figure 7). The external pressure h_{ext} (in centimeters of water depth), at the bottom of the column, is calculated by

$$h_{ext} = H + L + l_p \tag{19}$$

where $L = 55$ cm and $l_p = 0.2$ cm.

The value of h_{ext} is used for calculating the liquid water flux q_m through the porous plate (flux continuity through the porous plate and into the soil at the depth $z = L$ [lower boundary condition]; Table 2).

For the set of the outlined conditions, the system of the heat and mass conservation equations (Equations 1 and 4) was solved by using an implicit finite difference scheme with explicit linearization of the transport coefficients (Vauclin et al. 1979).

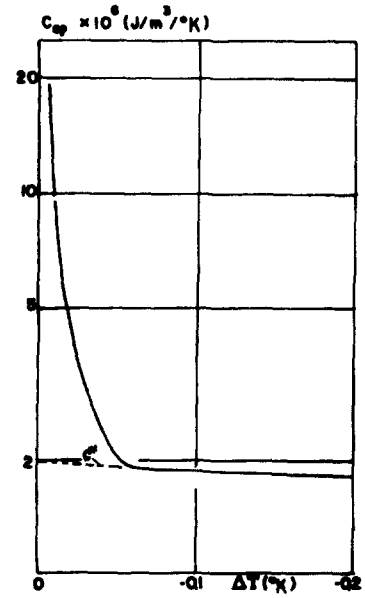

Figure 6 "Apparent" volumetric heat capacity versus freezing-point depression

Table 2 Experimental initial and boundary conditions

	Conditions	Hydraulic	Thermal
	Initial	$H(z) = -75$ cm	$T(z) = 294.16$k (21°C)
Test A	Boundary		
	U^a 0 cm	$q_m = 0$	T = 271.16K (−2°C)
	L^b 55 cm	$q_m = -a(h_{ext} - l_p - h_L)$	T = 294.16K (21°C)
	Initial	$H(z) = -65$ cm	T(z) = 296.16K (23°C)
B	Boundary		
	U^a 0 cm	$q_m = 0$	T = 271.16K (−2°C)
	L^b 55 cm	$q_m = -a(h_{ext} - l_p - h_L)$	T = 296.16K (23°C)

[a] Upper boundary (soil surface).
[b] Lower boundary (column's bottom).

The discretization of the system of equations was performed in the z, t plane with a very fine space increment in the region near the freezing front (isothermal of 273.16K). Moreover, small time steps were needed at the initial stages when the freezing front penetrated rapidly into the column. At each time step and at each depth in the frozen zone of the soil (T < 273.16K), the ice content change (Equation 1) was equal to the variation of the unfrozen water content Θ_1 corresponding to the freezing depression ΔT. The freezing front was assumed to be positioned midway between two adjacent depth nodes, the one node being in the frozen state (T < 273.16K) and the other in the unfrozen (T > 273.16K).

It should be noted that the effects of hysteresis (between infiltration and drainage), on the matric potential water content normalized functions $h^*(\Theta_1)$ (Figures 2a and 3a) have not been considered, and only the drainage curve was considered for describing the medium retention properties. This assumption was made for two reasons: (1) The initial moisture profile corresponding to either test A or test B was obtained after a drainage cycle, starting from soil's saturation (main drying). (2) During the freezing process, a permanent drying of the initial profile in the unfrozen zone was observed. In the frozen zone, the values of the cryogenic suction corresponding to the unfrozen water (Equation 11) are extremely high (Williams 1976). For instance, a temperature decrease ΔT of −1K yields −12.5 bars of cryogenic suction or −390.7 cm²/dyn (Equations 12 and 13). As can be seen from Figures 2a and 3a, this value is far beyond the range of hysteresis in the normalized matric potential functions, $h^*(\Theta_1)$.

The value of the exponent ω (Equation 16), necessary for estimating the hydraulic conductivity of the frozen soil, K_g, was selected equal to 8 (Vauclin et al. 1986).

For each experiment, the following simulations have been carried out:

1. The heat- and mass-transfer equations were solved simultaneously considering that the normalizations $h^*(\Theta_1)$ and $K^*(\Theta_1)$ were performed by means of the Gain factors G_h and G_k (Table 1; Equations T1.1 and T1.2; parameter set 1). Hereafter, this will be referred as $(H + M/GF)$ simulation.
2. The heat- and mass-transfer equations were solved simultaneously, assuming that $G_h = G_k = 1$ (Table 1; Equations T1.1 and T1.2; parameter set 2), hereafter referred as $(H + M/\text{STVF})$ simulation.
3. Only the heat-transfer equation was solved (hereafter referred as $[H]$ simulation).

Total moisture, Θ, and temperature, T, profiles along the soil column corresponding to tests A and B are illustrated in Figures 8a and b, and 9a and b, respectively. Additionally, in Figures 8c and d, and 9c and d are presented the cumulative volume of water entered into the column, V_1, and the freezing front location, Z_f, with respect to time. In all figures, the experimental data are represented by solid symbols. Solid lines represent the $(H + M/GF)$ simulated results, whereas dotted lines correspond to the results obtained by means of the $(H + M/\text{STVF})$ simulation. Finally, the dashed lines correspond to the (H) simulation results.

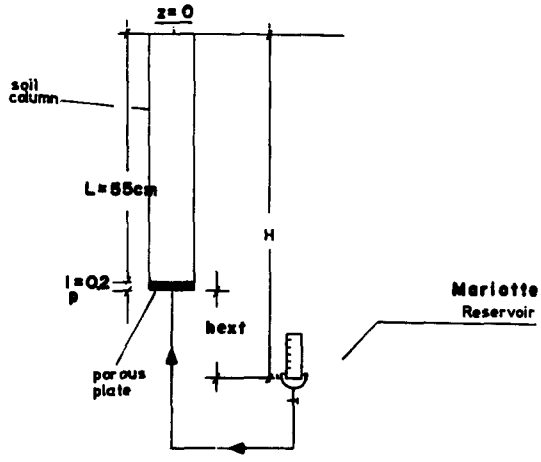

Figure 7 Hydraulic condition at the bottom of the column

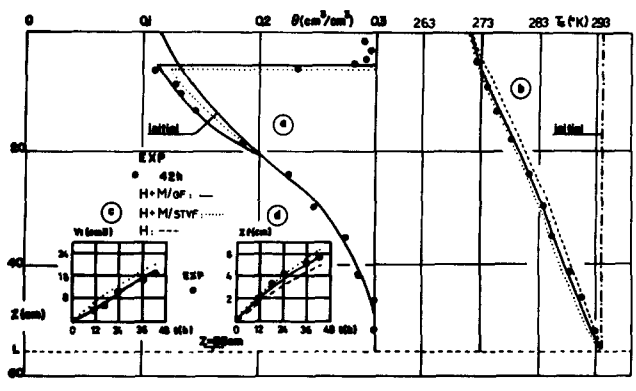

Figure 8 Numerical and experimental results for test A

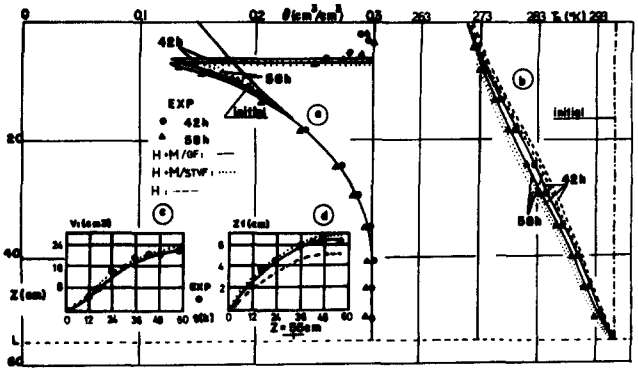

Figure 9 Numerical and experimental results for test B

The following comments can be made:

1. There is a good agreement between experimental and numerical results for both experimental tests, in the case of $(H + M/GF)$ simulation.

   On the contrary, the $(H + M/\text{STVF})$ simulated results overestimate persistently both the movement of the freezing front and the quantity of water migrating into the column. When only heat-transport equation is solved, the inverse effect is observed (i.e., underestimation of the position of the moving freezing front). For instance, in the case of test B, the total volume of liquid water entered into the column and the depth of the freezing front determined experimentally after 58 h are $V_l = 22\,\text{cm}^3$ and $Z_f = 6.3$ cm, respectively. These values are almost equal to those calculated by the $(H + M/GF)$ simulation (solid lines/Figures 9c and d). The corresponding values calculated at the same time by the $(H + M/\text{STVF})$ simulation are $V_l = 24\,\text{cm}^3$ and $Z_f = 7$ cm, respectively (dotted lines/Figures 9c and d), whereas the position of the freezing front computed via (H) simulation yields $Z_f = 5$ cm (dashed line/Figure 9d). Taking account of the scale of the physical model used (soil column), the magnitude of these discrepancies cannot be considered negligible when compared with real field conditions.

   These results demonstrate that the effect of mass transfer on the thermal state of soil is an important factor to be considered when simulating the freezing process in soil, because of the unavoidable interaction between frozen and unfrozen region, which is expressed mainly by means of the mass-transport equation.
2. Because the ice phase in the frozen soil acts as a sink for the liquid water, the freezing process through the simultaneous effects of thermal and hydraulic gradients induce a migration of liquid water from the water table to the frozen zone. This phenomenon is more profound in the case of test B, where the position of the water table (initial profile) is closer to the soil surface.
3. The moisture content in the unfrozen zone decreases sharply ahead of the freezing front, whereas, behind the freezing front the soil is at saturation conditions (i.e., volumetric unfrozen water and ice contents, $\Theta = \Theta_s$).

Conclusion

A simulation model was proposed for solving the problem of coupled heat and mass transfers in unsaturated soil during freezing. Comparison between the results of the proposed simulation model and experimental data obtained in a vertical soil column with the upper end subjected to a negative temperature showed that the model used can successfully describe the overall processes related to soil freezing, provided that both transport equations are solved simultaneously. For the soil type studied in this work (fine/medium sand), important discrepancies between experimental and numerical moisture and thermal profiles were observed, for the case of the heat and mass simulation including the STVF theory and also when the simulation is performed only with the heat-transfer equation.

Acknowledgments

The work reported on here was conducted during the author's stay in the Institute de Mecanique de Grenoble. Financial support of this research by AFME (Agence Française pour la Maitrise de l'Energie) is gratefully acknowledged. The author wishes to also thank Professors M. Vauclin and G. Vachaud for their guidance and their constructive suggestions.

References

Aguirre-Puente, J. and Fremond, M. 1975. Congelation d'un milieu poreux humide. Couplage des phenomenes elementaires, *C.R. Acad. Sci. Paris*, **281**, 377–380

Aguirre-Puente, J., Fremond, M. and Comini, G. 1978. Congelation des sols-etude physique et modeles mathematiques. *Int. J. Refrigeration*, **1**, 99–107

Aguirre-Puente, J. and Gruson, J. 1983. Measurement of permeabilities of frozen soils. *Fourth Int. Conference on Permafrost*, University of Alaska, Fairbanks, 1–13

Albergel, A. 1984. Étude experimentale et numerique des transferts de masse et de chaleur vers une zone gelee dans un sol partiellement sature. Ph.D. thesis, Universite Scientifique et Medicale de Grenoble, Grenoble, France

Burt, T. P. and Williams, P. J. 1976. Hydraulic conductivity in frozen soils. *Earth Surface Processes*, **1**, 349–360

Chahal, R. S. 1964. Effect of temperature and trapped air on the energy status of water in porous media. *Soil Sci.*, **98**, 107–112

Constantz, J. 1982. Temperature dependence of unsaturated hydraulic conductivity of two soils. *Soil Sci. Soc. Am. J.*, **46**, 466–470

De Vries, D. A. 1963. *Thermal Properties of Soils*, W. R. won Wijk (ed.). North Holland, Amsterdam

Fuchs, M., Campbell, G. S. and Papendick, R. I. 1978. An analysis of sensible and latent heat flow in a partially frozen unsaturated soil. *Soil Sci. Soc. Am. J.*, **42**, 379–385

Giakoumakis, S. G. 1984. Determination des parametres hydriques d'un sable en vue de l'étude de sa congelation. Memoire de DEA, INP Grenoble, France

Giakoumakis, S. G. 1987. Effets de la temperature sur les caracteristiques hydrodynamiques de deux sols non-satures indeformables: Contribution a l'étude de la propagation du gel. These de Docteur, INP Grenoble, France

Giakoumakis, S. G. and Tsakiris, G. P. 1991. Eliminating the effect of temperature from unsaturated soil hydraulic functions. *J. Hydrol.*, **129**, 109–125

Guymon, G. L. and Luthin, J. N. 1974. A coupled heat and moisture transport model for arctic soils. *Water Resour. Res.*, **10**, 995–1001

Haridasan, M. and Jensen, R. D. 1972. Effect of temperature on pressure head-water content relationship and conductivity of two soils. *Soil Sci. Soc. Am. Proc.*, **36**, 703–708

Harlan, R. L. 1973. Analysis of coupled heat-fluid transport in partially frozen soil. *Water Resour. Res.*, **9**, 1314–1323

Hesstvedt, E. 1964. The interfacial energy ice-water. *Norwegia Geotech. Inst.* (Publ. no. 56), 1–4

Hoekstra, P. 1966. Moisture movement in soils under temperature gradients with the cold-side temperature below freezing. *Water Resour. Res.*, **2**, 241–250

Hopmans, J. W. and Dane, J. H. 1986. Temperature dependence of soils hydraulic properties. *Soil Sci. Soc. Am. J.*, **50**, 4–9

Jame, Y. W. and Norum, D. I. 1980. Heat and mass transfer in a

freezing unsaturated porous medium. *Water Resour. Res.*, **16**, 811–819

Kay, B. D. and Groenevelt, P. H. 1974. On the interaction of water and heat transport in frozen and unfrozen soils. *Soil Sci. Soc. Am. Proc.*, **38**, 395–400

Kay, B. D., Sheppard, M. I. and Loch, J. P. G. 1976. A preliminary comparison of simulated and observed water redistribution in soils freezing under laboratory and field conditions. *Frost Action in Soils Int. Symposium*, University of Luleå, Sweden, **1**, 29–41

Kennedy, G. F. and Lielmez, J. 1973. Heat and mass transfer of freezing water-soil system. *Water Resour. Res.*, **9**, 395–400

Koopmans, R. W. R. and Miller, R. D. 1966. Soil freezing and soil water characteristic curves. *Soil Sci. Soc. Am. Proc.*, **30**, 680–685

Miller, R. D., Loch, J. P. G. and Bresler, E. 1975. Transport of water and heat in a frozen permeameter. *Soil Sci. Soc. Am. Proc.*, **39**, 1029–1036

Miller, R. D. 1980. Freezing phenomena in soils. *Applications of Soil Physics*, D. Hillel (ed.). Academic Press, New York

Morel-Seytoux, H. 1979. Mass and heat flow equations in soils under non-isothermal (including freezing) conditions. CER79-80-4JM24

Nimmo, J. R. and Miller, E. E. 1986. The temperature dependence of isothermal moisture versus potential characteristics of soils. *Soil Sci. Soc. Am. J.*, **50**, 1105–1113

Novak, V. 1975. Non-isothermal flow of water in unsaturated soils. *J. Hydrol. Sci.* (Polish Acad. Sci.), **2**, 37–51

Peck, A. J. 1960. Change of moisture tension with temperature and air pressure. *Theor. Soil Sci.*, **89**, 303–310

Philip, J. R. and De Vries, D. A. 1957. Moisture movement in porous materials under temperature gradients. *Trans. Am. Geophys. Union*, **38**, 222–232

Taylor, G. S. and Luthin, J. N. 1978. A model for coupled heat and moisture transfer during soil freezing. *Can. Geostech. J.*, **15**, 548–555

Vachaud, G. and Thony, J. L. 1971. Hysteresis during infiltration and redistribution in a soil column at different initial water contents. *Water Resour. Res.*, **7**, 111–127

Vauclin, M. and Giakoumakis, S. G. 1987. Coupled heat and mass transfers in partially saturated frozen soils: Experimental versus numerical results. *Com. AGU Fall Meeting*, San Francisco, USA, 6–11 December 1987

Vauclin, M., Giakoumakis, S. G., Gaudet, J. P. and Albergel, A. 1986. Experimental and numerical analysis of coupled heat and mass transfers in a partially saturated frozen soil. *XVIII Int. Symp. on Heat and Mass Transfer in Cryoengineering and Refrigeration*, Dubrovnick, **1**, 309–323

Vauclin, M., Haverkamp, R. and Vachaud, G. 1979. Resolution numerique d'une equation de diffusion non-lineaire: Application a l'infiltration de l'eau dans les sols non-satures. Presses Universitaires de Grenoble, Grenoble, France

Vauclin, M., Lagouarde, J. P., Thony, J. L., Hamburger, J. and Grausse, P. 1978. Determination du flux thermique conductif dans un sol non-sature a partir de mesures in-situ. *Proc. 6th Int. Heat Transfer Conference*, Toronto, Canada, **3**, 13–18

Wilkinson, G. E. and Klute, A. 1962. The temperature effect on the equilibrium energy status of water held by porous media. *Soil Sci. Soc. Am. Proc.*, **26**, 326–329

Williams, P. J. 1964a. Experimental determination of apparent specific heats of frozen soils. *Géotechnique*, **14**, 133–142

Williams, P. J. 1964b. Unfrozen water content of frozen soils and soil moisture suction. *Géotechnique*, **14**, 231–246

Williams, P. J. 1976. Thermodynamic conditions for ice accumulation in freezing soils. *Frost Action in Soils Int. Symposium*, University of Luleå, Sweden, **1**, 42–53